Polymer Journal (2018) 50:503–510
https://doi.org/10.1038/s41428-018-0042-x

ORIGINAL ARTICLE

Logic gate aggregation of poly(*N*-isopropylacrylamide) nanogels with catechol substituents that respond to body heat

Shingo Tamesue[1] · Shinji Abe[2] · Takuo Endo[2] · Takeshi Yamauchi[2,3]

Received: 19 October 2017 / Revised: 15 February 2018 / Accepted: 27 February 2018 / Published online: 4 April 2018

Abstract

Smart hydrogel materials are a popular topic of investigation because they have the potential to be used as smart drug carriers and soft actuators. Hydrogel materials showing responsiveness to logic gate-type stimuli are of special interest because their responsiveness can be regulated more accurately than that of common stimuli-responsive materials. In this study, poly(*N*-isopropylacrylamide) nanogels containing catechol substituents in their polymer network structure were prepared via precipitation polymerization. The prepared nanogels showed AND-type logic gate thermal aggregation behavior. The possible use of this logic gate-type smart nanogel aggregating system was investigated in a smart valve system.

Introduction

Many research groups have been enthusiastically studying nanogels and investigating their various functions [1–5] because these nanosized gel particles have the potential to be used in various applications, such as drug carriers [6], sensors [7], and catalysts [8]. For example, aggregated nanogels act as bulk materials and express functions that are inaccessible to dispersed nanogels [9, 10]. Therefore, if it is possible to regulate the aggregation and dispersion of nanogels smartly, new stimuli-responsive functional soft materials can be created. The poly(*N*-isopropylacrylamide) (PNIPAM) nanogel is one of the most popular nanogels because it demonstrates thermal responsiveness, such as size changes due to dehydration of the *N*-isopropylacrylamide substituents [11].

Some researchers have reported that nanogels, including PNIPAM nanogels, can be used as embolic materials; [12] controlling nanogel aggregation is important for this function. The preparation of nanogels that will aggregate in easily and accurately in a controlled manner would represent great progress in the field of nanogel-mediated embolic therapy.

In the human body, many molecules express stimuli-responsive functions [13–15]. However, this responsiveness is a complex combination of multiple stimuli-responsive processes that result in complicated and amazing functions. By mimicking the responsiveness of living systems, it will be possible to create better soft materials that can be used as drug carriers under very stringent conditions. Recently, many stimuli-responsive materials that mimic living systems, i.e., logic gate-type smart soft materials, have been reported [16–18]. For example, Hamachi et al. reported supramolecular hydrogel materials showing logic gate-type gel-sol phase transitions that respond to the reactions between enzymes and substrates [19].

Thus, we speculated that nanogels possessing logic gate-type aggregation properties could be very useful valve agents when their aggregation can be controlled extremely accurately.

The objective of this research was to construct a logic gate type nanogel aggregation system that is controllable

Electronic supplementary material The online version of this article (https://doi.org/10.1038/s41428-018-0042-x) contains supplementary material, which is available to authorized users.

✉ Shingo Tamesue
tamesue@eng.niigata-u.ac.jp

✉ Takeshi Yamauchi
yamauchi@eng.niigata-u.ac.jp

[1] Department of Applied Chemistry, Faculty of Engineering, Utsunomiya University, Yoko 7-1-2, Utsunomiya, Tochigi 321-8585, Japan

[2] Graduate School of Science and Technology, Niigata University, Ikarashi 2-8050, Nishi-ku, Niigata 950-2181, Japan

[3] Department of Material Science and Technology, Faculty of Engineering, Niigata University, Ikarashi 2-8050, Nishi-ku, Niigata 950-2181, Japan

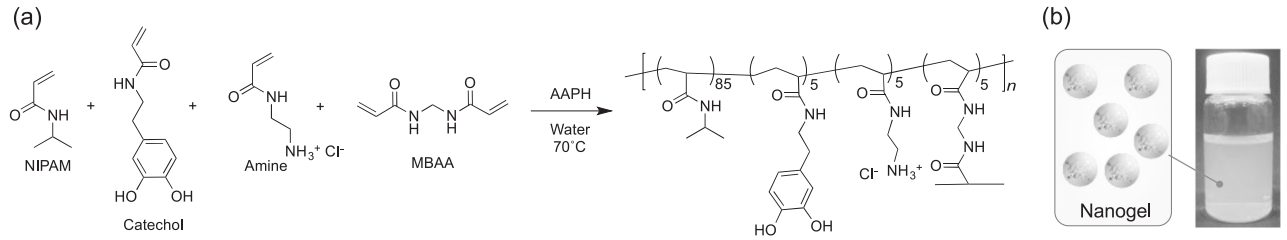

Fig. 1 (**a**) Synthetic scheme for catechol nanogel formation and (**b**) illustration and photograph of an aqueous dispersion a catechol nanogel

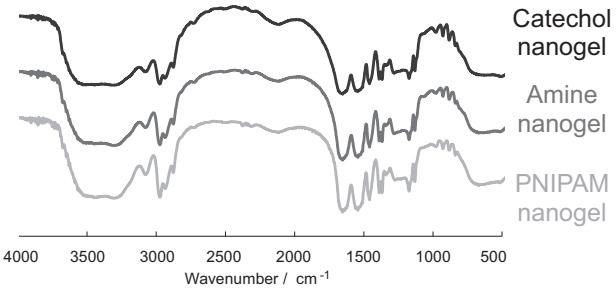

Fig. 2 FT-IR spectra (KBr) of a prepared catechol nanogel (blue), amine nanogel (red), and PNIPAM nanogel (green) (color figure online)

using heat. Moreover, we evaluated the possibility of using our aggregating system in smart valve systems.

Materials and methods

Experimental apparatus

N-Isopropylacrylamide (NIPAM), *N*,*N*'-methylenebis (acrylamide) (MBAA), acryloyl chloride, and 2,2′-azobis (2-aminopropane) dihydrochloride (AAPH) were purchased from Wako Pure Chemicals (Osaka, Japan). 3-Hydroxytyramine hydrochloride was purchased from the Tokyo Chemical Industry (Tokyo, Japan). Iron(III) chloride, anhydrous, was purchased from Kanto Chemicals. Triethylamine was purchased from Junsei Chemicals (Tokyo, Japan). All other chemicals and solvents were purchased from Kanto Chemical Co., Inc (Tokyo, Japan).

^{1}H NMR spectra were measured using Varian a 400 MHz spectrometer. ^{13}C NMR spectra were measured using a Varian 700 MHz spectrometer.

The average particle diameters of the nanogels were measured using a Shimadzu SALD-7100 nanoparticle size analyzer.

UV-vis spectra were measured using a 10 mm quartz cell in a Shimadzu UV-1800 spectrometer.

FT-IR spectra (KBr) were measured using a Shimadzu FTIR-8400S spectrometer.

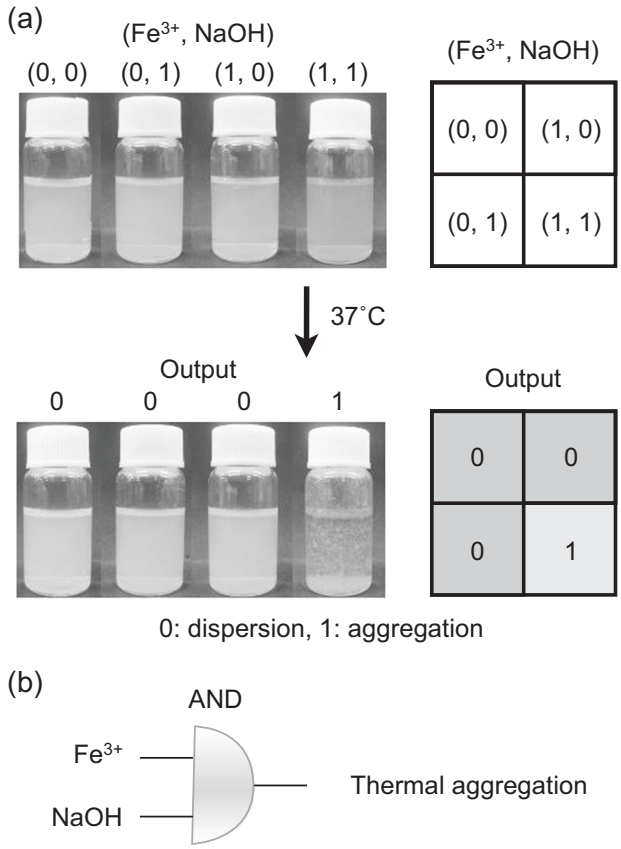

Fig. 3 (**a**) Photographs and truth tables of AND-type logic gate nanogel aggregation ([nanogel] = 0.05 wt%) at [Fe^{3+}] = 57.8 μM, [NaOH] = 0.2 M (pH = 13.2), and 37 °C. (**b**) Diagram of a heat-responsive AND-type logic gate nanogel aggregation

Digital microscope images were obtained using a Keyence VHX-900 microscope and scanning electron microscopy (SEM) images were obtained using a Jeol JCM-6000 scanning electron microscope.

The amine monomer shown in Fig. 1 was used to prepare the nanogels according to known literature procedures [20].

Catechol monomer

The catechol monomer, shown in Fig. 1, used to prepare the nanogels was synthesized according to known literature procedures [21].

Preparation of a nanogel with catechol substituents (catechol nanogel)

According to the synthetic scheme in Fig. 1a, NIPAM (2.89 g, 25.5 mmol), MBAA (231 mg, 1.50 mmol), and the amine monomer (226 mg, 1.50 mmol) were dissolved in deionized water (200 mL), and the solution was purged with nitrogen for 30 min. An aqueous solution of AAPH (163 mg, 120 mM, 5 mL), which had been purged with nitrogen for 30 min, was added dropwise to the solution in a four-neck separatory flask at 70 °C. The aqueous mixture was stirred at 250 r.p.m. for 30 min. Thereafter, an aqueous solution of catechol monomer (312 mg, 150 mM, 10 mL) was added to the solution. After 4 additional hours of stirring at 250 r.p.m. at 70 °C, the resultant nanogel was washed with deionized water (three times) via centrifugation (15×10^3 r.p.m., 10 °C) and collected. An aqueous dispersion of the catechol nanogel is shown in Fig. 1b.

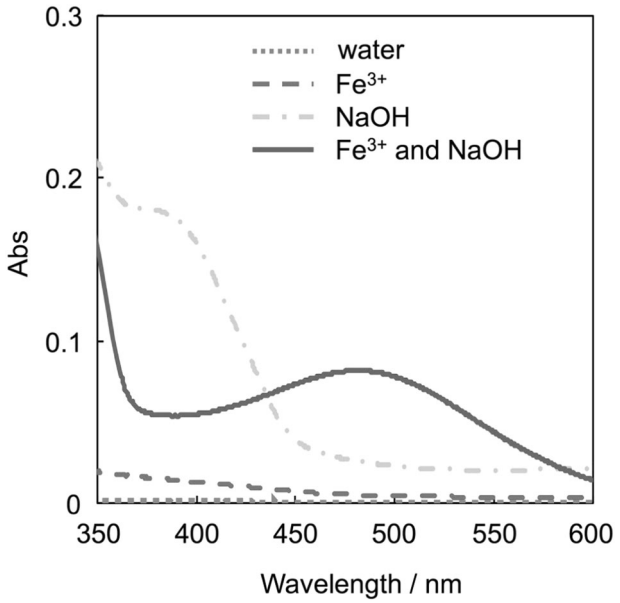

Fig. 4 UV-Vis spectra of the catechol monomer (60 μM) in deionized water before and after the addition of Fe^{3+} alone, NaOH alone, and both Fe^{3+} and NaOH ($[Fe^{3+}] = 20$ μM, [NaOH] = 0.2 M (pH = 13.2))

Preparation of the amine nanogel without catechol substituents (amine nanogel)

NIPAM (3.06 g, 27.0 mmol), MBAA (231 mg, 1.50 mmol), and the amine monomer (226 mg, 1.50 mmol) were dissolved in deionized water (200 mL), and the solution was purged with nitrogen for 30 min. An aqueous solution of AAPH (163 mg, 120 mM, 5 mL), which had been purged with nitrogen for 30 min, was added dropwise to the solution in a four-neck separatory flask, at 70 °C. The aqueous mixture was reacted for 4 h with stirring at 250 r.p.m. The resultant nanogel was washed with deionized water (three times) via centrifugation (15×10^3 r.p.m., 10 °C) and collected.

Preparation of the PNIPAM nanogel

NIPAM (3.23 g, 28.5 mmol) and MBAA (231 mg, 1.50 mmol) were dissolved in deionized water (200 mL), and the solution was purged with nitrogen for 30 min. An aqueous solution of AAPH (163 mg, 120 mM, 5 mL), which had been purged with nitrogen for 30 min, was added dropwise to the solution in a separatory flask at 70 °C. The aqueous mixture was allowed to react for 4 h with stirring at 250 r.p.m. The resultant gel particles were washed with deionized water (three times) via centrifugation (15×10^3 r.p.m., 10 °C) and collected.

IR spectra of the nanogels

The IR spectra of the prepared nanogels are shown in Fig. 2. All the nanogels showed amide I (C = O) and amide II (N–H) absorption peaks near 1680 and 1530 cm^{-1}, respectively.

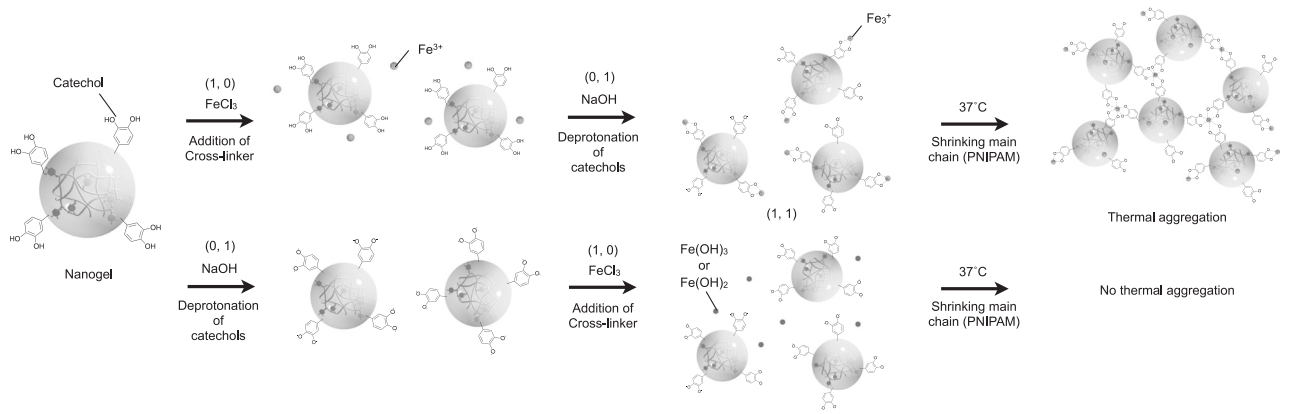

Fig. 5 Illustration depicting the AND-type logic gate nanogel aggregation caused by coordination bond formation between the diols of catechol and Fe^{3+} ions

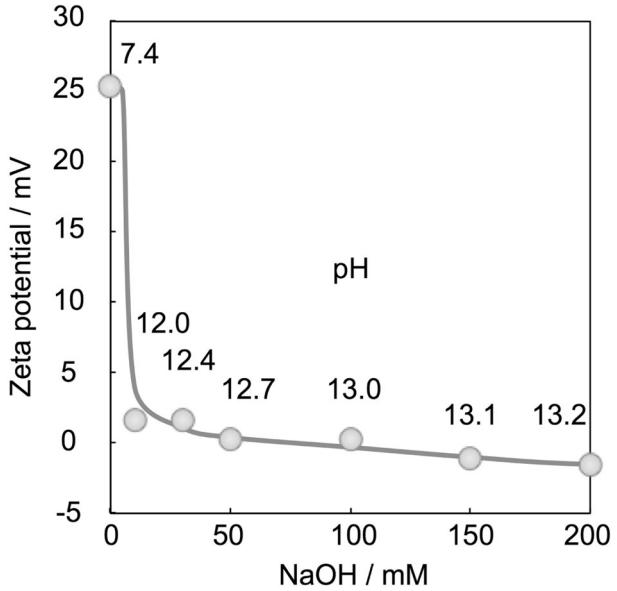

Fig. 6 Zeta potentials of catechol nanogel dispersions (0.05 wt%) containing Fe^{3+} (57.8 μM) and variable concentrations of NaOH (0–200 mM, pH = 7.4–13.2)

Results and discussion

In this study, we used nanogels containing catechol substituents (Fig. 1) prepared via radical precipitation polymerization as detailed in the Experimental Section. Catechol is one of the components in mussel tentacles that facilitates strong rock surface adhesion [22]. Many researchers have mimicked the strongly adhesive property of mussel tentacles by appending catechol to various functional materials [23, 24]. As stated in the introduction, catechols form coordination bonds to certain metal ions [25].

The prepared nanogels dispersed well in water, as shown in Fig. 1b, and we hypothesized that these nanogels could be used as strong adhesives, especially to glass, similar to mussel tentacles. However, unexpectedly, we found that these nanogels responded to Fe^{3+} and pH by aggregating.

The prepared nanogel dispersion (0.05 wt%) was mixed with aqueous $FeCl_3$, and then the pH was increased by the addition of NaOH ($[Fe^{3+}] = 57.8$ μM, [NaOH] = 0.2 M, pH 13.2). As seen in Fig. 3a and S1, the color of the aqueous dispersion changed from pale white to red due to the formation of coordination bonds between the catechol substituents and

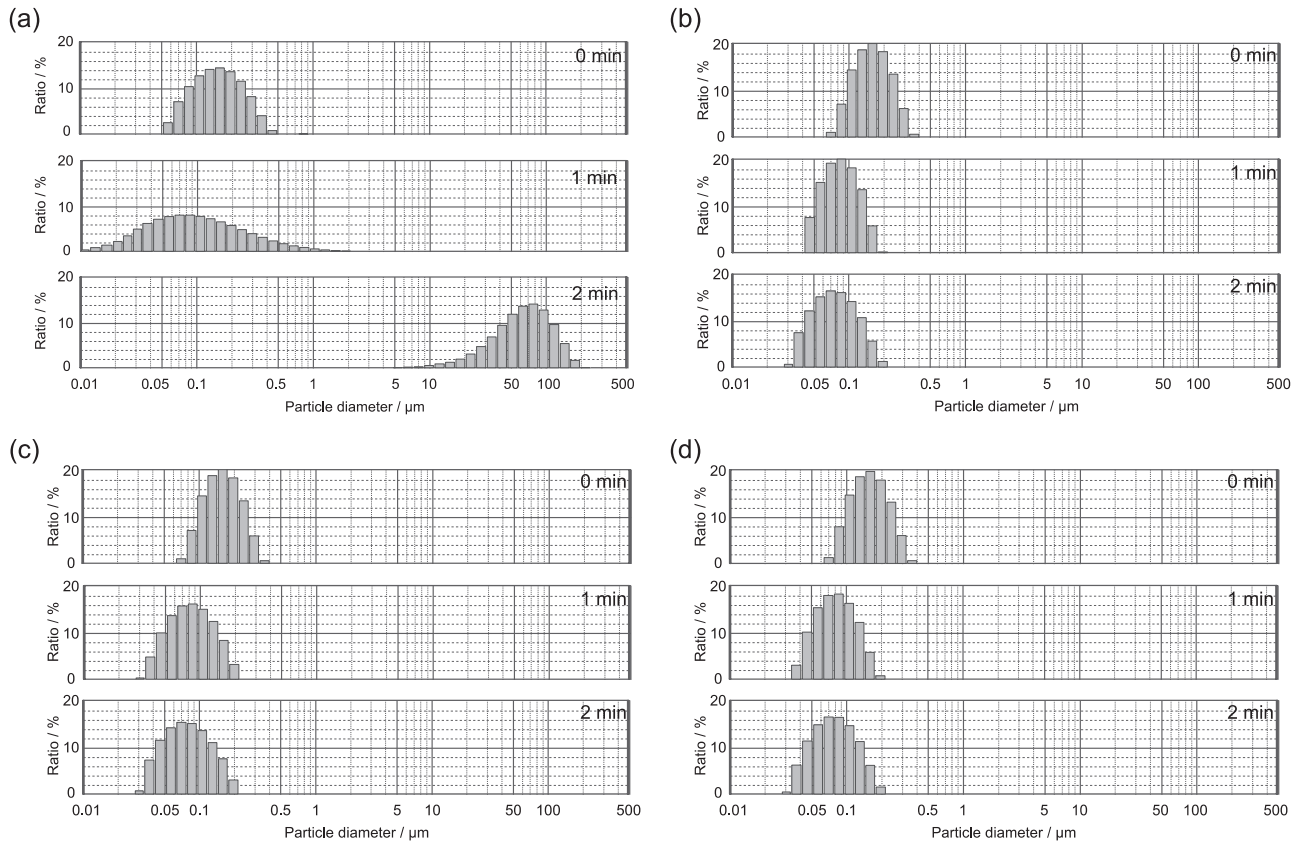

Fig. 7 Time course changes in the particle size distribution of the catechol nanogels at 37 °C: (**a**) nanogels (0.05 wt%) mixed with NaOH (0.2 M, pH = 13.2) and Fe^{3+} (57.8 μM), (**b**) nanogels (0.05 wt%) mixed with NaOH (0.2 M, pH = 13.2), (**c**) nanogels (0.05 wt%) mixed with Fe^{3+} (57.8 μM), and (**d**) nanogels (0.05 wt%) in water

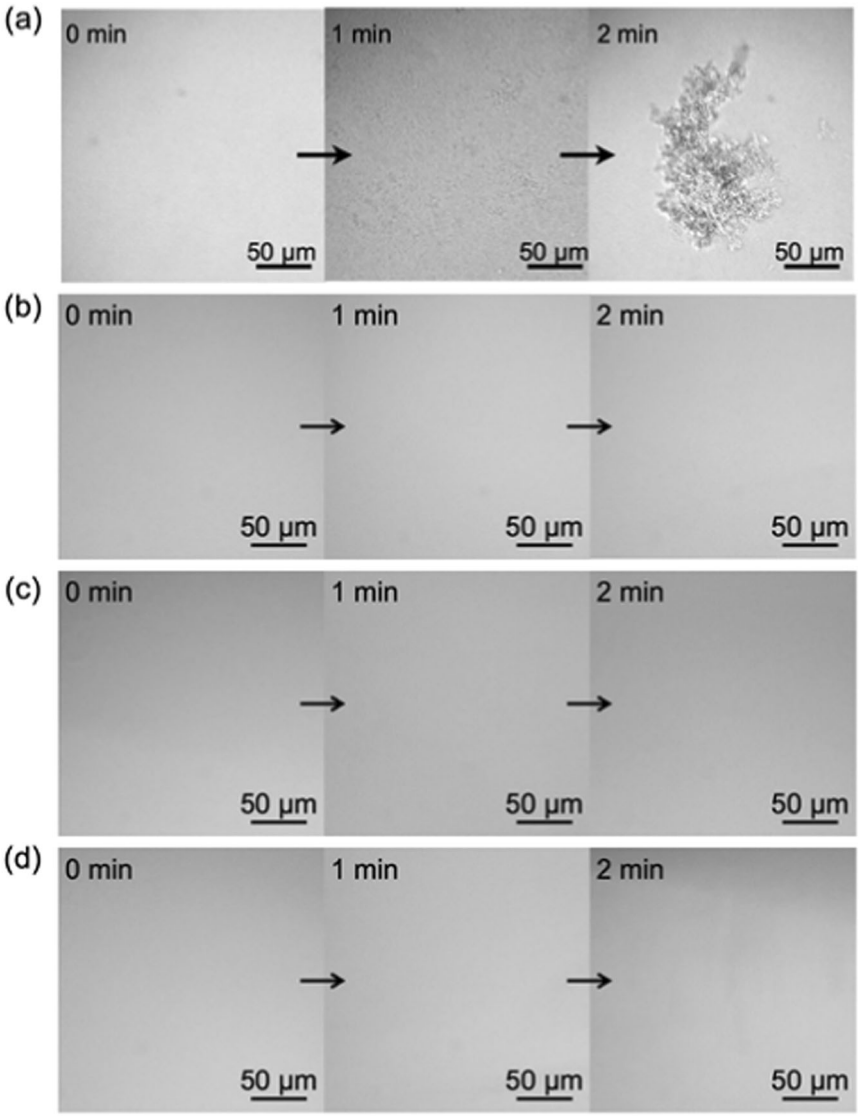

Fig. 8 Digital microscope images of time course changes in the nanogels (0.05 wt%) at 37 °C after 0–2 min on a glass slide: (**a**) nanogels mixed with NaOH (0.2 M, pH = 13.2) and Fe^{3+} (57.8 μM), (**b**) nanogels in water, (**c**) nanogels mixed with NaOH (0.2 M, pH = 13.2), and (**d**) nanogels mixed with Fe^{3+} (57.8 μM)

Fe^{3+} ions. After 1 min at 37 °C (human homeostatic body temperature), the nanogels that contained catechol substituents started to aggregate due to shrinkage of the NIPAM substituents. Finally, large aggregates were formed after 1.5 min. The precipitation timeframe was dependent on the nanogel concentration, Fe^{3+} concentration, and temperature.

On the other hand, nanogels that were not mixed with Fe^{3+} or were not in alkaline pH did not aggregate, even after heating. Similarly, nanogels without catechol substituents did not show the AND-type aggregation shown in Fig. 3b but thermally induced aggregation only at alkaline pH (pH 13.2). NaOH facilitates the dehydration of NIPAM because the hydrogen bonds between NIPAM and water molecules are cleaved at high pH. Additionally, no color changes were observed, as shown in Figure S2.

In addition, interestingly, it was found that the order in which $FeCl_3$ and NaOH are added into nanogels is important for the expression of thermal aggregation by the nanogels. When $FeCl_3$ was mixed into nanogels before the pH was increased by the addition of NaOH, the nanogels showed thermal aggregation. On the other hand, when NaOH was mixed into the nanogels before $FeCl_3$, the nanogels did not show thermal aggregation. It is considered that $FeCl_3$ converts into $Fe(OH)_3$ or $Fe(OH)_2$ before forming coordination bonds with catechol substituents when NaOH is mixed into nanogels before $FeCl_3$.

We also confirmed the color changes utilizing UV-vis spectroscopy, as shown in Fig. 4. No significant absorption bands were observed before the addition of Fe^{3+} and the pH increase nor after the addition of only Fe^{3+}. At alkaline pH (> 13), a small absorption band appeared near 400 nm. However, in the presence of Fe^{3+} and at alkaline pH, a strong absorption band near 490 nm was observed

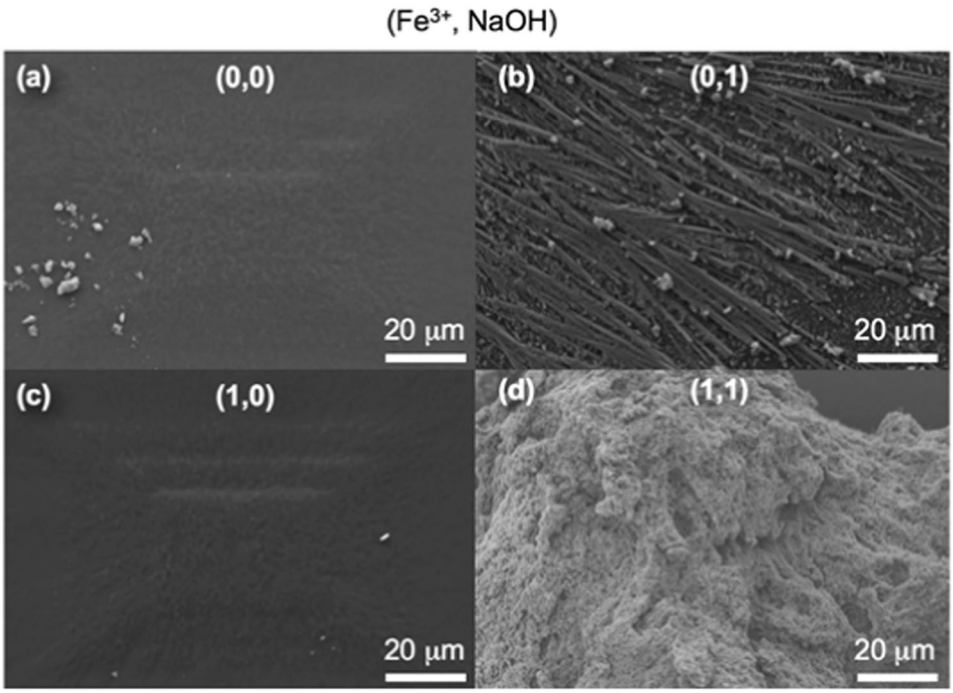

Fig. 9 SEM images of nanogels after heating at 37 °C: (**a**) nanogels (0.05 wt%) in water, (**b**) nanogels (0.05 wt%) mixed with NaOH (0.2 M, pH = 13.2), (**c**) nanogels (0.05 wt%) mixed with Fe^{3+} (57.8 μM), and (**d**) nanogels (0.05 wt%) mixed with NaOH (0.2 M, pH = 13.2) and Fe^{3+} (57.8 μM)

due to the formation of coordination bonds between the catechol diols and Fe^{3+}. None of the prepared nanogels aggregated in the presence of Fe^{3+} alone, even at 37 °C, because base-mediated deprotonation of the catechols is needed to form the coordination bonds and cross-link the nanogels.

Thus, the prepared nanogels demonstrated an AND-type logic gate response to Fe^{3+} and alkaline pH (Fig. 5). Alkaline pH is necessary for forming coordination bonds between catechol diols and Fe^{3+}, as shown in the zeta potentials of the nanogels under various pH conditions (Fig. 6), because deprotonation of the alcoholic protons is needed.

The particle size distributions of the nanogels under specific conditions are shown in Fig. 7. The average particle size of the nanogel mixed with Fe^{3+} at alkaline pH was ~153 nm before heating. After heating for 1 min, the particle size distribution decreased (100 nm). Since PNIPAM chains contract above their lower critical solution temperature, the nanogel shrank owing to this chain contraction. After 2 min, the average particle size increased more than 500 times the original average nanogel diameter to approximately 75 μm due to the formation of aggregates. In contrast, the average particle sizes of the nanogels mixed with Fe^{3+} ions or NaOH (approximately 159 nm and 158 nm, respectively) alone decreased and did not show significant increases, even after heating to 37 °C for 2 min, similar to the nanogels in pure water, as shown in Fig. 7b-d.

Digital microscope images of the nanogels are presented in Fig. 8. As evidenced in Fig. 8b, nanogel samples that were not mixed with Fe^{3+} and were not at alkaline pH were invisible under this magnification because the nanogel particle size was too small. Similar images were observed for the nanogel samples containing only Fe^{3+} at neutral pH or not containing Fe^{3+} at alkaline pH, as shown in Fig. 8d, c, respectively. However, large nanogel aggregates could be found extensively for the samples mixed with both Fe^{3+} and NaOH, as shown in Fig. 8a. The nanogel formed large, visible, aggregates under heating after the addition of both NaOH and Fe^{3+} because coordination bonds between the nanogels could be formed, leading to cross-linking.

The surface morphology of the prepared nanogel samples was observed by SEM (Fig. 9). Nanogels were cast onto carbon tape and spin-coated with Au. Large aggregated nanogels were observed only in the sample containing Fe^{3+} at alkaline pH, similar to that observed in the digital microscopy images in Fig. 8a. Only ionic salt crystals could be observed in all other nanogel samples.

Thus, the prepared nanogels aggregated only when the pH increased to alkaline values after Fe^{3+} had been added to the dispersion. This aggregation behavior is reflective of AND logic gate aggregation. A phase diagram is presented in Figure S5. This logic gate-type nanogel aggregation should be useful for the construction of soft actuators, in particular, smart nanogel valve systems. Therefore, we investigated this nanogel aggregation system as a valve system to regulate water flow.

Figure S3 shows a high concentration of the nanogels dispersed in water ([nanogel] = 1.0 wt%) before and after heating. Only the dispersion containing Fe^{3+} at alkaline pH

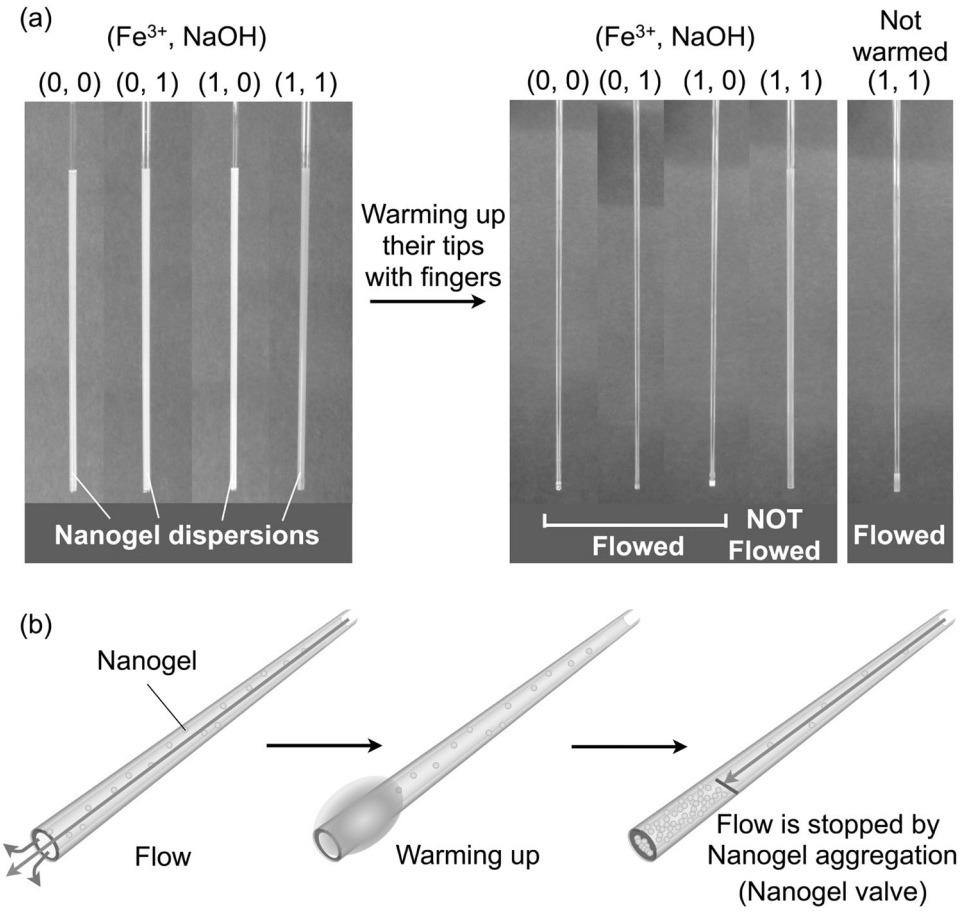

Fig. 10 (**a**) Photographs of flowing nanogel dispersions (1.0 wt%) in glass capillary tubes ($\varphi = 0.8$ mm) before and after warming the tubes using finger heat ($[Fe^{3+}] = 1.16$ mM, [NaOH] = 0.2 M, pH = 13.2). (**b**) Schematic illustration of water flow stoppage due to nanogel aggregation

($[Fe^{3+}] = 1.16$ mM, [NaOH] = 0.2 M, pH 13.2) formed a gel after heating. None of the other nanogels showed any significant phase transitions. This gelation behavior indicates that the nanogel polymer networks formed one large polymer network. This nanogel cross-linking through Fe^{3+} coordination enabled water retention and led us to design a water flow-regulating valve.

To investigate the possibility that our nanogel aggregation system could be applied as a valve system for regulating water flow smartly, nanogel dispersions (1.0 wt%) were placed in thin glass tubes ($\varphi = 0.8$ mm), and the flow of the dispersions from tube to tube was observed before and after heating (fingers used as the heat source), as shown in Fig. 10a and S4. All of the nanogel dispersions flowed out of the thin tubes under the influence of gravity. After warming the tips of the tubes, the nanogel dispersion containing Fe^{3+} at alkaline pH ($[Fe^{3+}] = 1.16$ mM, [NaOH] = 0.2 M, pH 13.2) stayed in the tubes. Thus, by partially warming the thin tube, the water flow could be controlled due to nanogel aggregation, as shown in Fig. 10b. This AND-type smart aggregation system indicates that the prepared nanogels have the potential to be used as smart valve systems for regulating water flow.

Conclusions

We prepared PNIPAM nanogels containing catechol substituents. The prepared nanogels showed body heat-induced aggregation behavior due to the formation of an AND-type logic gate response to Fe^{3+} and alkaline pH conditions. Moreover, we regulated water flow using this smart nanogel aggregation system in glass capillary tubes using only body heat (37 °C). We believe that this logic gate-type body temperature aggregation system may be useful for creating a new generation of smart valve systems that can regulate solvent flow, such as embolic agents. In its current state, the technology discussed in this paper cannot be applied to the human body. However, this study provides proof-of-concept for logic gate-type smart embolic agents compatible with the human body.

Acknowledgements This work was supported by JSPS Kakenhi (Grant Number: 17K14537) from the MEXT in Japan.

Compliance with ethical standards

Conflict of interest The authors declare that they have no conflict of interest.

References

1. Vinogradov SV, Bronich TK, Kabanov AV. Nanosized cationic hydrogels for drug delivery: preparation, properties and interactions with cells. Adv Drug Deliv Rev. 2002;54:135–47.
2. Oh JK, Drumright R, Siegwart DJ, Matyjaszewski K. The development of microgels/nanogels for drug delivery applications. Prog Polym Sci. 2008;33:448–77.
3. Kabanov AV, Vinogradov SV. Nanogels as pharmaceutical carriers: finite networks of infinite capabilities. Angew Chem Int Ed. 2009;48:5418–29.
4. Sasaki Y, Akiyoshi K. Nanogel engineering for new nanobiomaterials: from chaperoning engineering to biomedical applications. Chem Rec. 2010;10:366–76.
5. Xia L-W, Xie R, Ju X-J, Wang W, Chen Q, Chu L-Y. Nanostructured smart hydrogels with rapid response and high elasticity. Nat Commun. 2013;4:2226.
6. Ryu J-H, Chacko RT, Jiwpanich S, Bickerton S, Babu RP, Thayumanavan S. Self-cross-linked polymer nanogels: a versatile nanoscopic drug delivery platform. J Am Chem Soc. 2010;132:17227–35.
7. Gota C, Okabe K, Funatsu T, Harada Y, Uchiyama S. Hydrophilic fluorescent nanogel thermometer for intracellular thermometry. J Am Chem Soc. 2009;131:2766–7.
8. Lu A, Moatsou D, Longbottomb DA, O'Reilly RK. Tuning the catalytic activity of L-proline functionalized hydrophobic nanogel particles in water. Chem Sci. 2013;4:965–9.
9. Hu L, Sarker AK, Islam MR, Li X, Lu Z, Serpe MJ. Poly (N-isopropylacrylamide)microgel-based assemblies. J Polym Sci Part A. 2013;51:3004–20.
10. Hashimoto Y, Mukai S, Sawada S, Sasaki Y, Akiyoshi K. Advanced artificial extracellular matrices using amphiphilic nanogel-cross-linked thin films to anchor adhesion proteins and cytokines. ACS Biomater Sci Eng. 2016;2:375–84.
11. Duracher D, Elaissari A, Pichot C. Preparation of poly(*N*-isopropylmethacrylamide) latexes kinetic studies and characterization. J Polym Sci A. 1999;37:1823–37.
12. Zhao Y, Zheng C, Wang Q, Fang J, Zhou G, Zhao H, Yang Y, Xu H, Feng G, Yang X. Permanent and peripheral embolization: temperature-sensitive p(*N*-isopropylacrylamide-co-butyl methylacrylate) nanogel as a novel blood-vessel-embolic material in the interventional therapy of liver tumors. Adv Funct Mater. 2011;21:2035–42.
13. Mevissen TET, Kulathu Y, Mulder MPC, Geurink PP, Maslen SL, Gersch M, Elliott PR, Burke JE, van Tol BDM, Akutsu M, Oualid FE, Kawasaki M, Freund SMV, Ovaa H, Komander D. Molecular basis of lys11-polyubiquitin specificity in the deubiquitinase cezanne. Nature. 2016;538:402–5.
14. Cao E, Liao M, Cheng Y, Julius D. TRPV1 structures in distinct conformations reveal activation mechanisms. Nature. 2013;504:113–8.
15. Zhou A, Carrell RW, Murphy MP, Wei Z, Yan Y, Stanley PLD, Stein PE, Pipkin FB, Read RJ. A redox switch in angiotensinogen modulates angiotensin release. Nature. 2010;468:108–11.
16. Wang L, Lian W, Yao H, Liu H. Multiple-stimuli responsive bioelectrocatalysis based on reduced graphene oxide/poly(*N*-isopropylacrylamide) composite films and its application in the fabrication of logic gates. ACS Appl Mater Interfaces. 2015;7:5168–76.
17. Liu G-F, Ji W, Feng C-L. Installing logic gates to multiresponsive supramolecular hydrogel co-assembled from phenylalanine amphiphile and bis(pyridinyl) derivative. Langmuir. 2015;31:7122–8.
18. Xue P, Lu R, Jia J, Takafuji M, Ihara H. A smart gelator as a chemosensor: application to integrated logic gates in solution, gel, and film. Chem Eur J. 2012;18:3549–58.
19. Ikeda M, Tanida T, Yoshii T, Kurotani K, Onogi S, Urayama K, Hamachi I. Installing logic-gate responses to a variety of biological substances in supramolecular hydrogel–enzyme hybrids. Nat Chem. 2014;6:511–8.
20. Ma Y, Yung L-YL. Detection of dissolved CO_2 based on the aggregation of gold nanoparticles. Anal Chem. 2014;86:2429–35.
21. Sparks BJ, Hoff ET, Hayes LTP, Patton DL. Mussel-Inspired thiol–ene polymer networks: influencing network properties and adhesion with catechol functionality. Chem Mater. 2012;24:3633–42.
22. Kim HJ, Hwang BH, Lim S, Choi B-H, Kang SH, Cha HJ. Mussel adhesion-employed water-immiscible fluid bioadhesive for urinary fistula sealing. Biomaterials. 2015;72:104–11.
23. Maier GP, Rapp MV, Waite JH, Israelaachvili JN, Butler A. Adaptive synergy between catechol and lysine promotes wet adhesion by surface salt displacement. Science. 2015;349:628–32.
24. Nishida J, Kobayashi M, Takahara A. Light-triggered adhesion of water-soluble polymers with a caged catechol group. ACS Macro Lett. 2013;2:112–5.
25. Kim BJ, Oh DX, Kim S, Seo JH, Hwang DS, Masic A, Han DK, Cha HJ. Mussel-mimetic protein-based adhesive hydrogel. Biomacromolecules. 2014;15:1579–85.